Transition-State Structure and Reactivity in the Acid–Base-Catalyzed Hydrolysis of a Model Intermediate for Corn-Plant Herbicide Resistance[1]

Naomi I. Nakano, Masahiro Kise,[2] Edward E. Smissman,[3] Katherine Widiger, and Richard L. Schowen*

Department of Medicinal Chemistry, School of Pharmacy, and Department of Chemistry, University of Kansas, Lawrence, Kansas 66045

Received August 12, 1974

The intermediate formed by nucleophilic displacement of chloride from the herbicide Cyprazine (2-chloro-4-isopropylamino-6-cyclopropylamino-*s*-triazine) by *N*-hydroxysuccinimide undergoes hydrolysis with a complex pH dependence. The data are consistent with reactant, present in protonated, neutral, and anionic forms, undergoing addition of water to the aromatic ring to generate an intermediate compound which decomposes in acid-catalyzed, uncatalyzed, and base-catalyzed processes. Transition-state acidities and the absolute and relative activation parameters suggest activated complex structures which are highly aromatic. This is in contrast to the conventional expectation that these species should resemble the unstable intermediate. This apparent violation of Hammond's postulate may signal the intervention of kinetically significant solvent-reorganization processes.

The herbicide Cyprazine (2-chloro-4-isopropylamino-6-cyclopropylamino-*s*-triazine) is detoxified by the corn plant through a nonenzymatic nucleophilic displacement of chloride ion by a naturally present benzoxazinone hydroxamic acid glucoside to form compound 1H. This compound is then hydrolyzed to a water-soluble hydroxytriazine (eq 1) which is excreted.[4] We showed previously[4] that formation of the model compound 2H from Cyprazine and *N*-hydroxysuccinimide involved an extremely reactant-like transition state with catalytic proton bridging between substrate and nucleophile moieties. It was also demonstrated that the mechanistic principles uncovered could account quantitatively for observations on in vivo detoxification by corn plants.

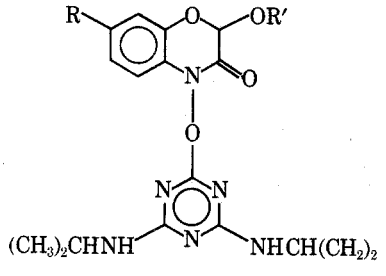

1H

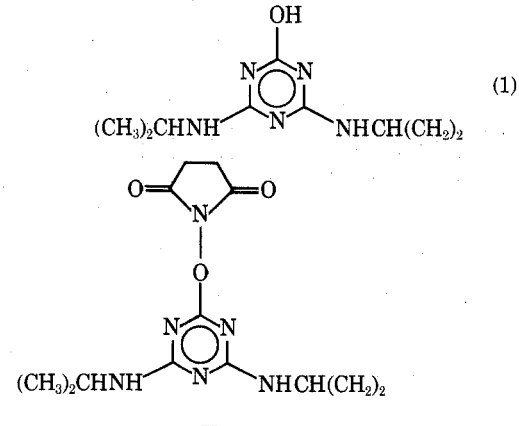

(1)

2H

We now turn our attention to the conversion of 2H to the hydroxytriazine through the agency of water, acids, and bases. 2H is a very highly functionalized molecule and it is not difficult to generate mechanisms for the hydrolysis reaction. Perhaps the simplest and most attractive from the viewpoint of biological economy is nucleophilic displacement by water or water-derived species (eq 2), which would regenerate the intact resistance factor in vivo. Another important possibility, however, is offered by the opening of the imide ring and a subsequent Lossen rearrangement (eq 3). This route would mean loss of the resistance factor in the course of herbicide destruction and would indicate that heavy application of herbicide might override the natural resistance of the corn plant.

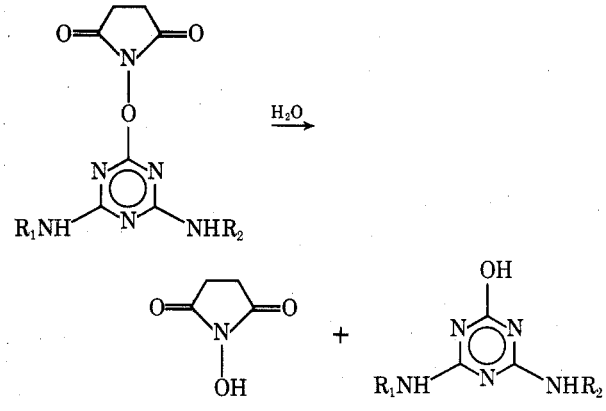

3 4 (2)

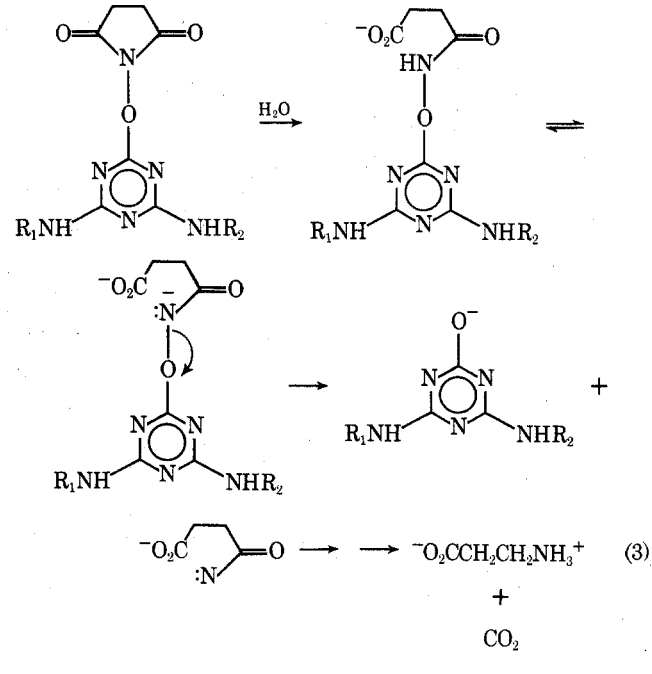

(3)

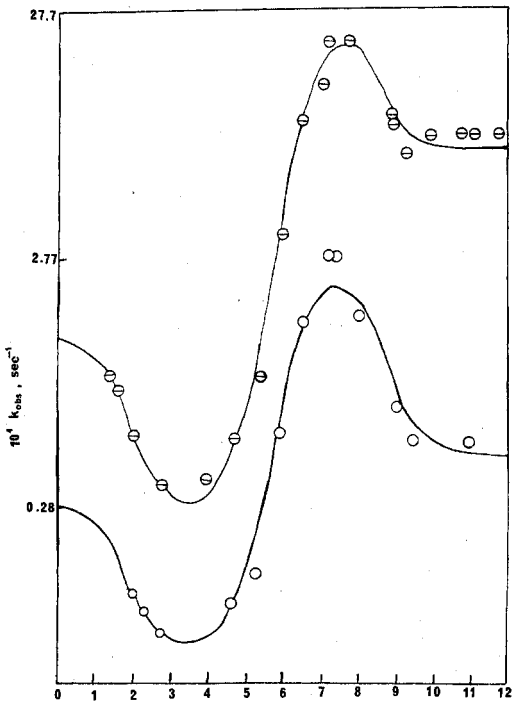

Figure 1. Dependence of the observed rate constant for hydrolysis of 2H on the pH of the solution at 70° (upper curve) and 50° (lower curve). Data are given in Table I.

This paper reports a characterization of the mechanistic routes from 2H to the hydroxytriazine and a discussion of their significance for transition-state structure in this reaction class.

Results

Reaction Products. Analysis of the reaction products as described in the Experimental Section showed only the hydroxytriazine 4 and *N*-hydroxysuccinimide (3) to be present at pH's of 2.50, 7.00, and 11.00. This excludes the mechanism of eq 3 and supports that of eq 2.

Kinetics. Table I shows first-order rate constants for the hydrolysis of 2H at various pH's at temperatures of 70 and 50°. These rate constants can be described by eq 4, the parameters of which will be discussed below. The calculated rate constants given in Table I are those from eq 4 with the parameters exhibited in Table II; graphical comparisons of the experimental and calculated pH dependences are presented in Figure 1. Although the curve fitting is unsophisticated, it produces data of sufficient reliability for the solution of the problems considered in this paper. Table II also contains the values of the enthalpies and entropies of activation calculated from the Eyring equation.[5]

$$k_{obsd} = \frac{k_1[H^+] + k_2K_a}{K_a + [H^+]} + \frac{k_ak_eK_w[H^+]}{(K_a' + [H^+])(k_a[H^+] + k_ek_w)} + \frac{k_bK_a'}{K_a' + [H^+]} \quad (4)$$

Acidity of 2H. Spectrophotometric titration of 2H at 220 nm yielded a pK_a of 8.4 ± 0.1, presumably for loss of a proton from a side-chain NH function. This is in satisfactory agreement with pK_a' = 8.5, found from fitting eq 4 to the data of Table I.

Discussion

The mechanism of Scheme I is a reasonable manifold of processes and is consistent with eq 4 under the assumptions given below. Figure 2 shows a diagrammatic version

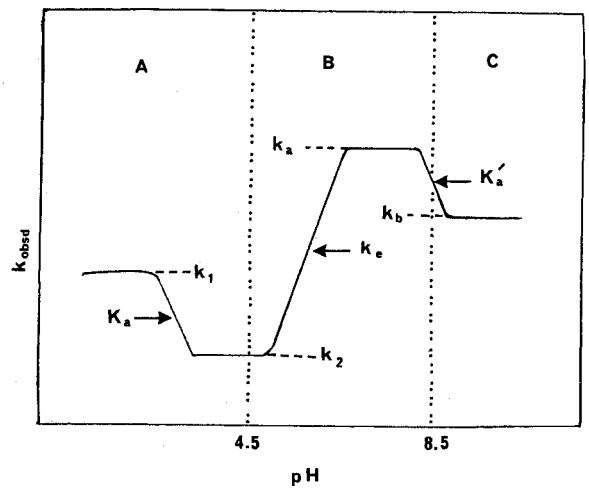

Figure 2. Schematic division of the pH dependence of Figure 1 into region A (below pH 4.5), region B (pH 4.5–8.5), and region C (above pH 8.5). Rate and equilibrium constants are those of eq 4.

of the pH–rate profiles of Figure 1, illustrating that they are divisible into three distinct regions, labeled A, B, and C. We consider these in turn.

Scheme I

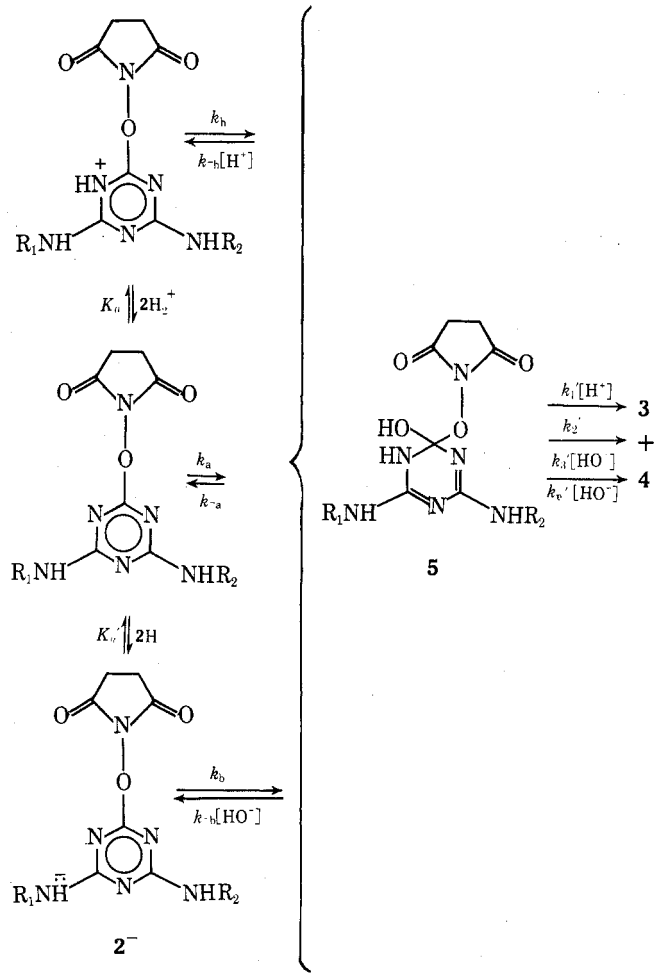

Region A. Only $2H_2^+$ and 2H are present as reactants, interconnected by pK_a = 1.5. Both generate 5 in rapid, reversible processes (k_h and k_a). The slow decomposition of 5 by the k_1' and k_2' routes is then rate limiting. When reactant is primarily $2H_2^+$, only the k_1' decomposition path is important; when reactant is primarily 2H, only the k_2' path is observed. Then

Table I
First-Order Rate Constants for Hydrolysis of 3×10^{-4} *M* 2H in Water as a Function of pH at 70.00 ± 0.05° (μ = 0.50 *M*)[a]

$10^5 k_{obsd}$, sec^{-1} (pH) 70°	$10^5 k^b_{calcd}$, sec^{-1} 70°	$10^5 k_{obsd}$, sec^{-1} (pH) 50°	$10^5 k^b_{calcd}$, sec^{-1} 50°
9.77 (1.38)	9.75	1.31 (2.12)	1.33
8.44 (1.60)	8.31	1.08 (2.41)	1.10
5.50 (2.07)	5.55	0.92 (2.82)	0.94
3.50 (2.74)	3.50	1.18 (4.64)	1.10
3.72 (3.94)	3.25	1.53 (5.29)	2.15
5.42 (4.70)	4.94	5.55 (6.00)	6.44
9.56 (5.38)	12.8	16.2 (6.60)	14.4
35.2 (6.01)	39.4	29.7 (7.25)	20.9
99.7 (6.60)	102	29.2 (7.51)	21.7
140 (7.13)	167	17.0 (8.12)	19.1
212 (7.30)	181	6.97 (9.10)	8.86
208 (7.85)	195	5.19 (9.48)	6.67
103 (8.98)	114	4.97 (11.0)	4.75
96.9 (8.99)	114		
72.5 (9.35)	95.0		
83.6 (10.0)	80.0		
86.9 (10.8)	76.1		
86.9 (11.1)	76.1		
88.6 (11.8)	76.1		

[a] Ionic strength maintained by addition of KCl. pH's are correct at indicated temperatures and were maintained by acetate, phosphate, Tris, and carbonate buffers or adjusted by addition of hydrochloric acid or sodium hydroxide. Rate constants are reproducible to within ±5%.

$$k^A_{obsd} = \frac{[H^+]}{K_a + [H^+]} \frac{k_h}{k_{-h}} k_1' + \frac{K_a}{K_a + [H^+]} \frac{k_a}{k_{-a}} k_2' \quad (5)$$

Defining $k_h k_1'/k_{-h} = k_1$ and $k_a k_2'/k_{-a} = k_2$, we have eq 6. Note that this is the first term of eq 4.

$$k^A_{obsd} = \frac{k_1[H^+] + k_2 K_a}{K_a + [H^+]} \quad (6)$$

Region B. Only 2H is present through most of the region but begins to ionize to 2^- at higher pH. The k_e' route of elimination dominates all others and becomes so fast at about pH 7 that the rate-determining step changes to the k_a step. Including the correction for ionization of 2H, we have

$$k^B_{obsd} = \frac{[H^+] k_a k_e' [HO^-]}{(K_a' + [H^+])(k_{-a} + k_e'[HO^-])} \quad (7)$$

Multiplying numerator and denominator by k_a/k_{-a}, defining $k_a k_e'/k_{-a} = k_e$, and converting from hydroxide to hydrogen-ion concentrations yields eq 8, which is the second term of eq 4.

$$k^B_{obsd} = \frac{k_a k_e K_w [H^+]}{(K_a' + [H^+])(k_a[H^+] + k_e K_w)} \quad (8)$$

Region C. The conversion of 2H to 2^-, by the process of $pK_a' = 8.5$, is now completed and the rate finally levels off at high pH as water attack on 2^- becomes dominant. Thus

$$k^C_{obsd} = \frac{K_a' k_h}{K_a' + [H^+]} \quad (9)$$

Equation 9 is the third term of eq 4.

The mechanistic recapitulation is thus as follows. In region A, at pH < ~2, $2H_2^+$ rapidly and reversibly is converted to 5, which then expels *N*-hydroxysuccinimide with acid catalysis. Since reactants and transition state are both uni-

Table II
Rate Constants in the Hydrolysis of 2H at 70.00 ± 0.05° and 50.00 ± 0.05° and Values of the Corresponding Activation Parameters

Constant,[a,b] dimensions	70°	50°	$\Delta H^\ddagger$, kcal/mol	$\Delta S^\ddagger$, eu
$10^4 k_1$, sec^{-1}	1.42	0.31	16 ± 1	−30 ± 3
$10^5 k_2$, sec^{-1}	2.78	0.78	14 ± 1	−40 ± 3
$10^3 k_a$, sec^{-1}	2.36	0.25	24 ± 1	0 ± 3
$10^4 k_b$, sec^{-1}	7.22	0.36	32 ± 1	+20 ± 3
$10^{-3} k_e$, M^{-1} sec^{-1}	2.71	1.47	6 ± 1	−25 ± 3

[a] Although errors in individual rate constants were not calculated, the root mean square deviation from the curves shown in Figure 1 is about 15% of the root mean square data point. [b] Equilibrium constants used with these rate constants to fit eq 4 were pK_a = 1.5 (70 and 50°), pK_a' = 8.5 (70 and 50°), and pK_w = 12.8 (70°), 13.3 (50°) ("Handbook of Chemistry and Physics", 54th ed, R. C. Weast, Ed., Chemical Rubber Publishing Co., Cleveland, Ohio, 1973, p D-131; the value for 70° was extrapolated).

positive, the rate is pH independent. As the pH is decreased, $2H_2^+$ goes over to 2H, which is also rapidly and reversibly converted to 5. At the same time the acid-catalyzed route of elimination gives way to an uncatalyzed pathway. Now both reactants and transition state are electrically neutral and again the rate becomes pH independent (pH 3–4).

Beyond pH 4 the base-catalyzed decomposition of 5 comes into play and the rate rises with pH. Near pH 7, the decomposition rate surpasses the velocity of formation of 5 from 2H and the latter becomes rate determining. Again the rate loses its pH dependence. However, shortly beyond pH 8, the conversion of 2H to 2^- sets in and the rate begins to drop. This continues to around pH 9–10 when the reaction of water with 2^- to form 5 (which rapidly decomposes) becomes observable.

Accessibility of Transition States. Scheme II shows how we are able to study the properties of five different

Scheme II

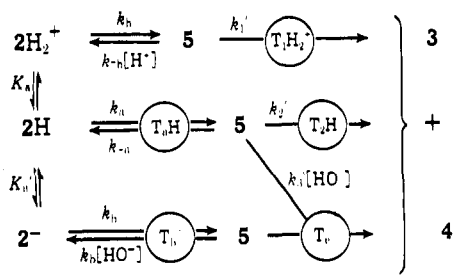

transition states in this system. In pH region A, we can measure the rate constants k_1 and k_2, which contain information about the transition states $T_1H_2^+$, for acid-catalyzed breakdown of intermediate 5 to products, and T_2H, for uncatalyzed breakdown (eq 10 and 11). In pH region B,

$$H_2O + 2H_2^+ \xrightarrow{k_1} T_1H_2^+ \quad (10)$$

$$H_2O + 2H \xrightarrow{k_2} T_2H \quad (11)$$

we obtain values for k_e and k_a, illuminating transition states T_e^- for base-catalyzed breakdown of 5 and T_aH for addition of water to 2H to form 5, respectively (eq 12 and

$$HO^- + 2H \xrightarrow{k_e} T_e^- \quad (12)$$

$$H_2O + 2H \xrightarrow{k_a} T_aH \quad (13)$$

13). Finally, in pH region C, k_b is measured allowing investigation of transition state T_b^- for addition of water to 2^- (eq 14).

$$H_2O + 2^- \xrightarrow{k_b} T_b \qquad (14)$$

It should be kept in mind that the free energy of activation is a state function, so that the rate constants represent *overall* transformations from initial state to transition state and do not contain information about the *route* followed by reacting species between initial and transition states. Thus, for example, any number of rapid proton transfers or heavy-atom reorganizations may in principle intervene between the reactant structures on the left-hand sides and the transition-state structures on the right-hand sides of eq 10–14. We shall resist the temptation, at least initially, to speculate about the detailed routes of transition-state generation and concentrate on transition-state *structures* only.

Transition-State Structural Proposals. We suggest that the structures of the five transition states investigated in this study are those shown in **6–10.** These structures are supported by (a) the transition-state acidities;[6] (b) the absolute values of the entropies of activation; and (c) the relative values of the enthalpies and entropies of activation. The arguments are given below; they have in common that fairly gross effects are involved so that precise rate-constant values are not needed.

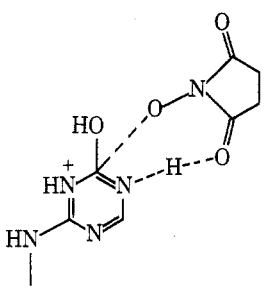

6($T_1H_2^+$)

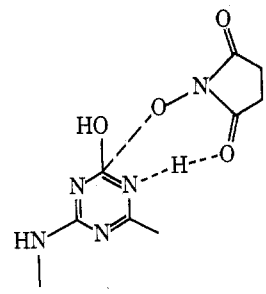

7(T_2H)

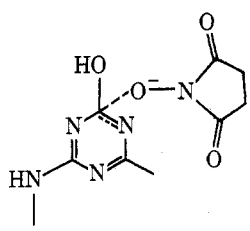

8(T_e^-)

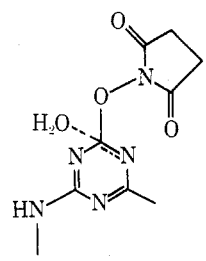

9(T_aH)

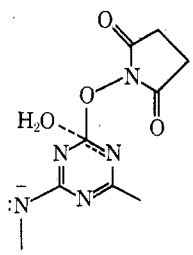

10(T_b^-)

The feature possessed alike by all of these transition-state structures is that they do *not* resemble the intermediate adduct **5.** Rather the transition states between **5** and products (**6, 7,** and **8**) strongly resemble the products in having a nearly intact aromatic ring structure, with the bond to the leaving group nearly broken. Likewise, the transition states between reactants and **5** (**9** and **10**) closely favor the reactants, with nearly intact aromatic rings and entering-group bonds very weak. This runs counter to conventional thought about reactions involving unstable intermediates, where the Hammond postulate is usually taken to imply that transition states leading to and from such transient, unstable species as **5** should resemble it closely.[7]

Transition states $T_1H_2^+$ and T_2H are also postulated to contain the catalytic proton bridge between ring-nitrogen and leaving-group carbonyl which was found for the attack of *N*-hydroxysuccinimide on a chlorotriazine substrate.[4] This is reasonable since the steps in which these transition states are observed in this system are models for the microscopic reverse of nucleophilic attack on the chlorotriazine. Furthermore, the bridge is supported by the experimental observations in this case.

We now proceed to present the lines of evidence favoring structures **6–10.** First, we discuss transition-state acidities; second, the entropies of activation; and third, the relative activation parameters.

Transition-State Acidities. Because $\Delta G^\ddagger$ is a state function, we can define free energies of interconversion among different activated complexes (whether or not such interconversions occur under actual conditions). Kurz has used this idea to good avail.[6] For our present purpose, we use the thermodynamic cycles of eq 15–17, with data for 50°.

$$\begin{array}{ccc} 2H_2^+ & \xrightarrow{k_1 = 10^{-4.5}} & T_1H_2^+ \\ \downarrow{\scriptstyle K_a = 10^{-1.5}} & & \downarrow{\scriptstyle K_{12}^*} \\ 2H + H^+ & \xrightarrow[k_2 = 10^{-5.1}]{} & T_2H + H^+ \end{array} \qquad (15)$$

$$\begin{array}{ccc} 2H & \xrightarrow{k_a = 10^{-3.6}} & T_aH \\ \downarrow{\scriptstyle K_{a'} = 10^{-8.5}} & & \downarrow{\scriptstyle K_{ab}^*} \\ 2^- + H^+ & \xrightarrow[k_b = 10^{-4.4}]{} & T_b^- + H^+ \end{array} \qquad (16)$$

$$\begin{array}{ccc} HO^- + H^+ + 2H & \xrightarrow{k_2 = 10^{-5.1}} & T_2H + H^+ + HO^- \\ \downarrow{\scriptstyle k_e = 10^{3.2}} & & \downarrow{\scriptstyle K = 10^{13.3}} \\ H^+ + T_e^- & \xrightarrow[K_{2e}^*]{} & T_2H + H_2O \end{array} \qquad (17)$$

The cycle of eq 15 allows us to calculate K_{12}^*, the acidity constant for conversion of $T_1H_2^+$ to $T_2H + H^+$. If $T_1H_2^+$ closely resembles $2H_2^+$ and T_2H closely resembles 2H in having intact aromatic rings (the change of OH for the leaving group should have little effect), as suggested in structures **6** and **7,** then K_{12}^* should be nearly equal to K_a^*, the acidity constant for conversion of $2H_2^+$ to $2H + H^+$. On the other hand, if $T_1H_2^+$ resembled the protonated form of **5** and T_2H were structurally similar to **5** itself, then K_{12}^* should be near the ionization constant for the ring NH of **5.** This pK is probably[4] about 12. From eq 15, we find $pK_{12}^* = 1.5 + 5.1 - 4.5 = 2.9$. This value is far closer to 1.5 than to 12 and strongly supports the structural hypotheses of **6** and **7.**

Correspondingly, the value of K_{ab}^* from the cycle of eq

16 tests the postulate that T_aH and T_b^- structurally approximate 2H and 2^-, respectively, as advanced in structures **9** and **10**. pK_a' for ionization of 2H to 2^- is 8.5, while pK_{ab}^* is 9.3. These values are quite close, and pK_{ab}^* supports structures **9** and **10**. If the aromatic structure had been lost in T_aH and T_b, as it would have been had they resembled **5**, then pK_{ab}^* should have been much larger.

Finally, the cycle of eq 17 yields K_{2e}^* for ionization of T_2H to T_e^-. This provides information on the catalytic bridging proton in T_2H and $T_1H_2^+$, which is the proton released in this ionization. As we see from eq 17, $pK_{2e}^* = 5.0$. Now if this proton had been simply attached to the ring nitrogen and not in a bridging situation, we would have expected a pK a bit higher than that of $2H_2^+$ (1.5), perhaps about 2.9 as found for $T_1H_2^+$ above. Instead, the much lower acidity found shows that the proton is stabilized in place by the catalytic bridge.

In summary, the ionization of $T_1H_2^+$ to T_2H has about the same free-energy change as ionization of $2H_2^+$ to 2H. Also, the ionization of T_aH to T_b^- has about the same free-energy change as ionization of 2H to 2^-. These results show that the aromatic structure which is largely responsible for the acid–base properties of $2H_2^+$, 2H, and 2^- is essentially intact in $T_1H_2^+$, T_2H, T_aH, and T_b^-. Furthermore, the ionization of T_2H to T_e^- is relatively difficult, as expected from stabilization of the bridging proton in T_2H.

Entropies of Activation. Formation of $T_1H_2^+$ and T_2H from 2H involves large losses of entropy ($\Delta S^\ddagger = -30$ and -40 eu, respectively). This is consistent with structures **6** and **7** because (a) complete addition of a water molecule should have reduced the entropy, perhaps by 5–10 eu,[8] and (b) formation of the cyclic nucleophilic–protolytic bifunctional-catalytic bridge structure should have resulted in considerable further loss of internal rotational entropy. The bridging may also have prevented any effective gain of entropy from loosening of the leaving group oxygen–carbon bond.

Conversion of 2H to T_aH results in no change in entropy, fully consistent with the suggestion in **9** that only the loosest kind of association has formed with the nucleophilic water (thus little loss of translational and rotational entropy) and that no charges have developed, which would have reduced the entropy from electrostriction of solvent. The corresponding reaction of 2^- generating T_b^- actually produces an increase in entropy ($\Delta S^\ddagger = +20$ eu). This may indicate that the nucleophilic water (loosely bound as in **10**) was originally a member of the extensive solvation shell of the negative charge so that no entropy loss was associated with its weak binding to the substrate carbon. The entropy gain may be connected with a gain in rotational freedom of the leaving group as the nucleophile begins to prevent conjugation of its oxygen lone pairs into the ring, and with some disruption of the highly ordered reactant solvation shell. The same gain in leaving group rotational freedom in T_aH may also cancel some small entropy loss as the nucleophile begins to bind.

The production of T_e^- from 2H and HO^- is a second-order reaction and exhibits an apparently normal $\Delta S^\ddagger$ of -25 eu. However, as we shall see below, this actually is higher (more positive) than expected on the basis of the low $\Delta H^\ddagger$, and the discrepancy supports the loose bond to the leaving group shown in **8**.

Relative Activation Parameters. Enthalpy–Entropy Relation. Figure 3 shows a plot of $\Delta H^\ddagger$ vs. $\Delta S^\ddagger$ for each of the processes studied. For four of the five processes, the variations in $\Delta H^\ddagger$ are strongly correlated with the changes in $\Delta S^\ddagger$ as indicated by the line drawn through the points. The slope of the line, the isergonic ("isokinetic") temperature, is 300 K although the strict linearity of the relationship is unimportant for our purposes. Only the general fact that large decreases in $\Delta H^\ddagger$ are accompanied by large decreases in $\Delta S^\ddagger$ is relevant.

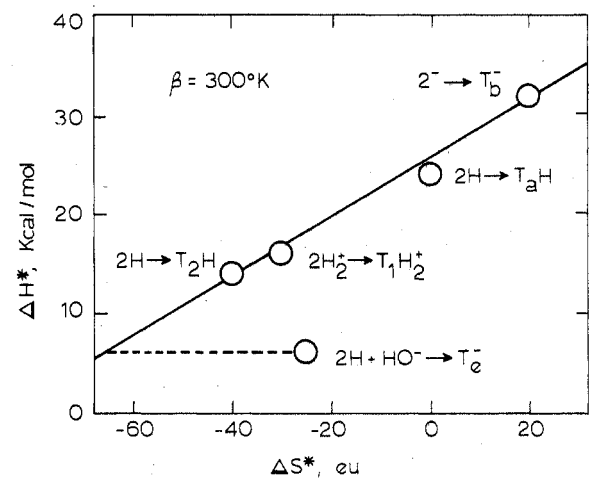

Figure 3. Relationship of the enthalpy of activation ($\Delta H^\ddagger$) to the entropy of activation ($\Delta S^\ddagger$) for the various activation processes.

The processes leading to transition states T_aH and T_b^- exhibit quite large $\Delta H^\ddagger$ with $\Delta S^\ddagger$ either zero or positive. It is these transition states which are proposed (in **9** and **10**) to involve incipient attack on the aromatic ring, possibly with some increased freedom of motion of the leaving group (as O lone-pair conjugation to the ring is interrupted) and possibly some solvent-shell disruption. No special stabilizing interactions are present.

Formation of transition states $T_1H_2^+$ and T_2H, in which catalytic proton bridging is proposed (**6** and **7**), occurs with far less energy expenditure. Indeed, if the difference in $\Delta H^\ddagger$ between this pair of transition states and the T_aH–T_b^- pair represents the stabilization from catalytic bridging, the enthalpic contribution from this source is about 13 kcal/mol. This would produce a rate acceleration of around 10^{10}-fold if it were not offset by an unfavorable shift of about 55 eu in $\Delta S^\ddagger$. Presumably this arises from the loss of internal vibrational freedom as the leaving group is locked into the cyclic bridging structure. The large entropy loss suggests a reasonably rigid stereochemical requirement for the bifunctional interaction of the leaving group.

Finally we note that if formation of T_e^- had followed the tendency of the other processes, its very small $\Delta H^\ddagger$ of 6 kcal/mol would have produced a $\Delta S^\ddagger$ of less than -60 eu (see dashed line on Figure 3). This would not have been expected on the basis of structure **8**, however. The low $\Delta H^\ddagger$ here is not a reflection of catalytic bridging but of complete bond formation by the powerful nucleophile hydroxide ion. In fact, the leaving group is now presumably nearly broken free; the resultant freedom of internal motion presumably accounts for the relatively positive $\Delta S^\ddagger$.

Hammond's Postulate Violation. We noted above that the general experience of mechanisms science, as summarized in Hammond's postulate, is that transition states leading to and from unstable intermediates such as **5** should resemble the intermediates structurally, rather than reactants or products. We found the contrary here, with every accessible transition state having a nearly intact aromatic ring, like reactants or products but unlike the nonaromatic **5**. Several explanations are possible.

One ready explanation might seem to be that there is no intermediate and that the displacement is concerted. However, the interpretation offered above for the break in the pH–rate profile at pH 7 (region B) is that the rate-deter-

Scheme III

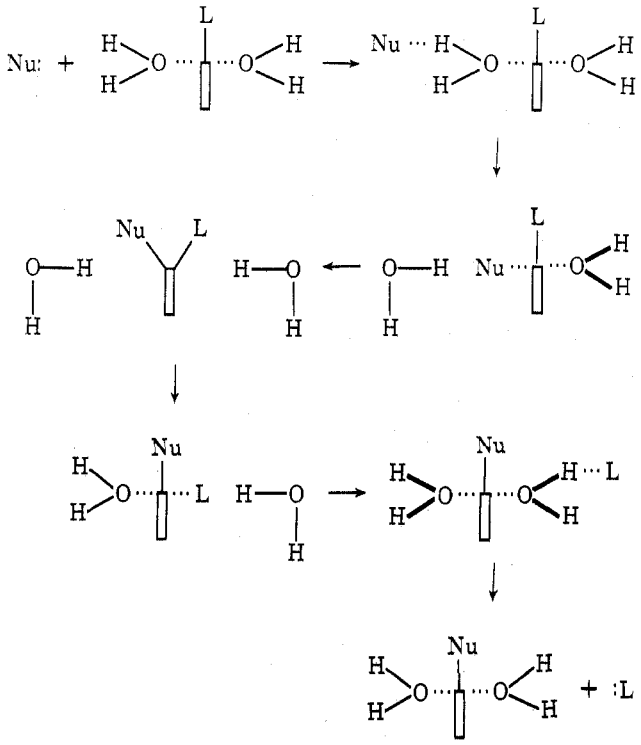

mining step changes at this pH. This constitutes kinetic evidence for an intermediate compound and thus casts doubt on this explanation.

A more likely view is that some other higher energy intermediates, having intact aromatic rings, intervene before and after **5**. For example, consider the sequence of Scheme III, which corresponds to the well-established course of events in the solvolysis reactions of alkyl derivatives.[9] In Scheme III, Nu: represents a nucleophile displacing the leaving group L: from an aromatic ring. Species which correspond to the intimate and solvent-separated ion pairs of solvolysis are shown. These are kinetically significant in solvolysis and their formation and decomposition are sometimes rate determining. If such is the case here, clearly the aromatic ring would remain intact in the transition state. However, even if the covalent-bond formation or fission steps are still rate limiting, conversion of a high-energy desolvated intermediate ("intimate ion pair") to the adduct **5** might well have a transition-state structure resembling the desolvated intermediate. Indeed, this would follow from Hammond's postulate.

Thus the apparent violation of Hammond's postulate may signal the intervention of kinetically significant solvent-reorganization processes along the main reaction path.

Experimental Section

Kinetics. Reaction rates were measured by following the first-order change in absorbance at 243 nm, as described previously.[4]

pK_a of Substrate. Starting material in methanol stock solution was diluted 50-fold with aqueous buffers to a final concentration of 1.5×10^{-5} *M*. Buffers controlled the pH at 6.32–9.58 and consisted of phosphate, Tris, carbonate, and sodium hydroxide solutions. The change in absorbance at 220 nm was used to determine a pK_a of 8.3–8.5.

Reaction Products. Reaction products were determined by thin layer chromatography. Samples were spotted on precoated silica gel F-254 plates (Brinkmann Instruments) and developed to a distance of 7 cm with two solvent systems: A [1-butanol–acetic acid–water (5:1:4)] and B [isopropyl alcohol–ammonia–water (80:5:15)]. These systems gave R_f values (A followed by B) of 0.74 and 0.44 for the starting material, 0.60 and 0.56 for 2-hydroxy-4-isopropylamino-6-cyclopropylamino-*s*-triazine ("hydroxy product"), and 0.41 and 0.11 for *N*-hydroxysuccinimide. Only these materials were detectable in reaction solutions after several days. Products were determined at pH 2.50 (solution of starting-material hydrochloride), 7.00, and 11.00 (adjusted with sodium hydroxide). Use of SilicAR TLC-7G (Mallinckrodt Chemical Works) plates resulted in the same findings.

Registry No.—2H, 54643-26-4.

References and Notes

(1) This research was supported by grants from the National Institutes of Health (NS 09399 and GM 18017) and the National Science Foundation. Data reduction was carried out in part in the Computation Center of the University of Kansas.
(2) On leave from the Nippon Shinyaku Co., Ltd., Kyoto, Japan.
(3) Dr. Smissman died on July 14, 1974.
(4) N. I. Nakano, E. E. Smissman, and R. L. Schowen, *J. Org. Chem.*, **38**, 4396 (1973), and references cited therein.
(5) A. A. Frost and R. G. Pearson, "Kinetics and Mechanism", 2nd ed, Wiley, New York, N.Y., 1961, pp 98–99.
(6) J. L. Kurz, *Acc. Chem. Res.*, **5**, 1 (1972).
(7) G. S. Hammond, *J. Am. Chem. Soc.*, **77**, 334 (1955).
(8) L. L. Schaleger and F. A. Long, *Adv. Phys. Org. Chem.*, **1**, 1 (1963).
(9) V. J. Shiner, Jr., in "Isotope Effects in Chemical Reactions", C. J. Collins and N. S. Bowman, Ed., Van Nostrand-Reinhold, Princeton, N.J., 1970, Chapter 2, and references cited therein.